

# The Chemical Structure of Medium-Scale Pool Fires

Ryan Falkenstein-Smith, Kunhyuk Sung, Jian Chen, and Anthony Hamins,  
National Institute of Standards and Technology, Gaithersburg, MD 20899-8664, USA

## 1. Introduction

Use of fire modeling, such as the Fire Dynamic Simulator<sup>1</sup>, in fire protection engineering has increased dramatically during the last decade due to the development of practical computational fluid dynamics fire models and the decreased cost of computational power. Today, fire protection engineers use models to design safer buildings, nuclear power plants, aircraft cabins, trains, and marine vessels to name a few types of applications. To be reliable, the models require validation, which involves an extensive collection of experimental measurements. An objective of this report is to provide data for use in fire model evaluation by the research community.

A pool fire is a fundamental combustion configuration of interest in model development. In pool fires, the fuel surface is isothermal, flat and horizontal, which provides a well-defined and straightforward setup for testing models and furthering the understanding of fire phenomena. In moderate and large-scale pool fires, radiative heat transfer is the dominant mechanism of heat feedback to the fuel surface. Species concentrations and temperatures have a significant influence on the radiative heat transfer. A zone of particular interest is the fuel rich-core between the flame and the pool surface, where gas species can absorb energy that would otherwise have been transferred to the fuel surface. Few studies in the literature studies have reported local chemical species measurements, which provide a deep understanding of the chemical structure of a pool fire and provide insight on critical kinetic, heat, and mass transfer processes.

The purpose of this study is to characterize the spatial distribution of stable gas-phase chemical species in a moderate-scale liquid pool fire steadily burning in a well-ventilated quiescent environment. Here, methanol is selected as the fuel. Fires established using methanol are unusual as no carbonaceous soot is present or emitted. This creates a particularly useful testbed for fire models and radiation sub-models that consider emission by gaseous species - without the confounding effects of blackbody radiation from soot.

In this study, measurements are made in a 0.30 m diameter methanol pool fire. This particular fire was selected for study since the measurements complement the results from previous studies, including analyses of the mass burning rate, the temperature and velocity fields, radiative emission, flame height, and pulsation frequency<sup>2-3</sup>. Additional characterization of this fire enables a more comprehensive understanding of its detailed structure, enhancing the understanding of fire physics.

## 2. Experimental Method

The experimental setup used in this work has been documented previously<sup>3-6</sup>. Experiments were conducted under a canopy hood surrounded by a 2.5 m x 2.5 m x 2.5 m enclosure made of a double-mesh screen wall. The walls of the enclosure were formed by a double layer of wire-mesh screen (5 mesh/cm) that reduced the influence of compromising room flows that could disrupt the pool fire's flow field. All measurements were made once the burning conditions, specifically the mass burning rate, reached steady-state, achieved approximately 10 min after ignition.

## 2.1 Pool Burner

A circular, stainless-steel pan with an outer diameter of 0.30 m, a depth of 0.15 m, and a wall thickness of 0.0016 m was used as the pool burner. The burner was placed within an overflow basin, which extended 3 cm beyond the burner wall. The burner was fitted with legs such that the burner rim was positioned 0.3 m above the ground. The bottom of the burner was maintained at a constant temperature by flowing water ( $20\text{ }^{\circ}\text{C} \pm 3\text{ }^{\circ}\text{C}$ ) through a 3 cm section on the bottom of the fuel pan.

While burning, the fuel level was monitored by a camera with a zoom lens to allow visual observations, displayed on a 50 cm monitor, of the barely discernible dimple made from the fuel-level indicator on the fuel surface. The fuel level indicator was positioned near the center of the burner as shown in Figure 1. To preserve a consistent mass burning rate, the fuel level was maintained 10 mm below the burner rim, following conditions used in previous studies. Fuel to the burner was gravity fed from a reservoir positioned on a mass load cell located outside the enclosure and monitored by a data acquisition system. The fuel flow was manually adjusted using a needle valve. The expanded uncertainty with a coverage factor of 2 of the fuel level was estimated to be 0.5 mm for these experiments.

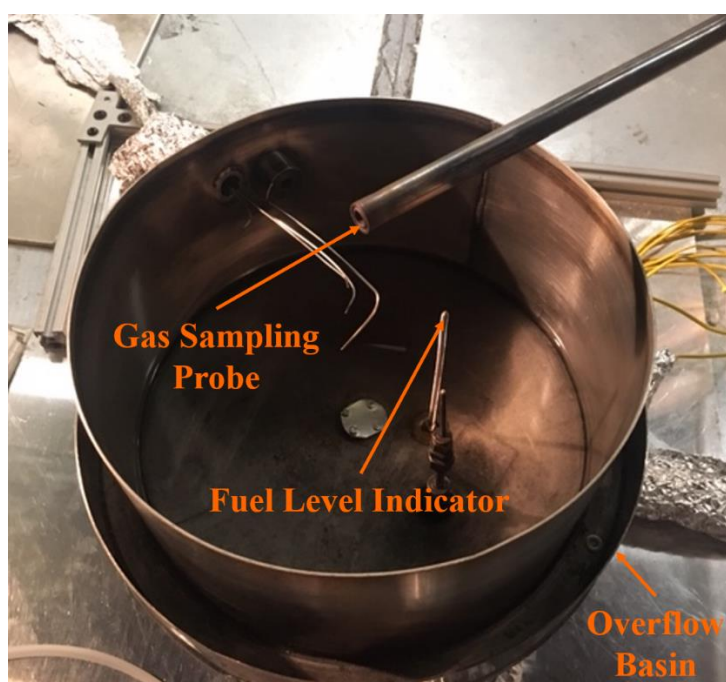


**Figure 1.** Pool Burner, 30 cm in diameter, with fuel level indicator, overflow section, and quenching probe

## 2.2 Gas Species Measurement

Gas-species measurements were made using an Agilent 5977E Series Gas Chromatograph/Mass Spectrometer System (GC/MS) fitted with a thermal conductivity detector (TCD).<sup>\*</sup> The GC/MS was able to quantify a variety of stable reactants, intermediates, and combustion product species collected from the pool fire. The GC was configured with a 2 ml sampling loop. Chromatographic separation of species was achieved using a Select for Permanent Gases-Dual Column (CP7430) comprised of mole-sieve and Porapak Q columns working in parallel and using a helium carrier gas. The sample analysis time was 33 min wherein the carrier gas flow leading into the TCD and MS was 3.0 ml/min and 1 ml/min, respectively. During the analysis, the GC oven temperature was maintained at 30°C for 10 min, then ramped at 8°C/min for 20 min until a temperature of 190°C was obtained.

---

<sup>\*</sup> Certain commercial products are identified in this report in order to specify adequately the equipment used. Such identification does not imply recommendation by the National Institute of Standards and Technology, nor does it imply that this equipment is the best available for the purpose.

Figure 2 displays the flow diagram for gas sampling into the GC/MS. After achieving steady-state burning conditions, a vacuum pump, located downstream from the GC/MS, was initiated. Gas samples were collected using a quenching probe. The quenching probe was composed of two concentric, stainless-steel tubes with outer annular coolant flow and inner, extracted, gas-sample flow. The inner and outer tube diameters were 7.9 mm and 16 mm, respectively. Water maintained at 90°C was used to flow through the sampling probe for the duration of the experiment. The remainder of the sampling line leading into the GC was heated with electrical, heating tape to prevent condensation of water and methanol through the line.

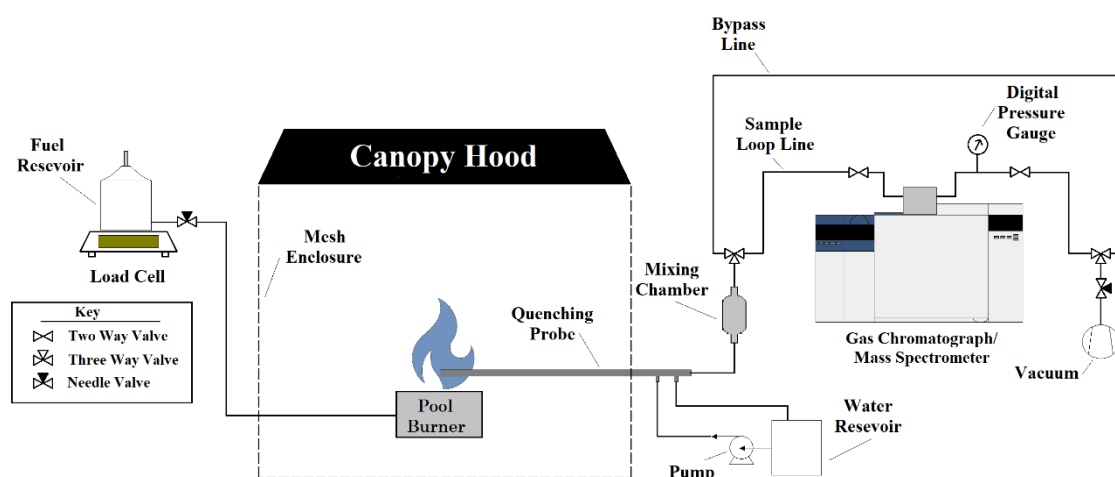
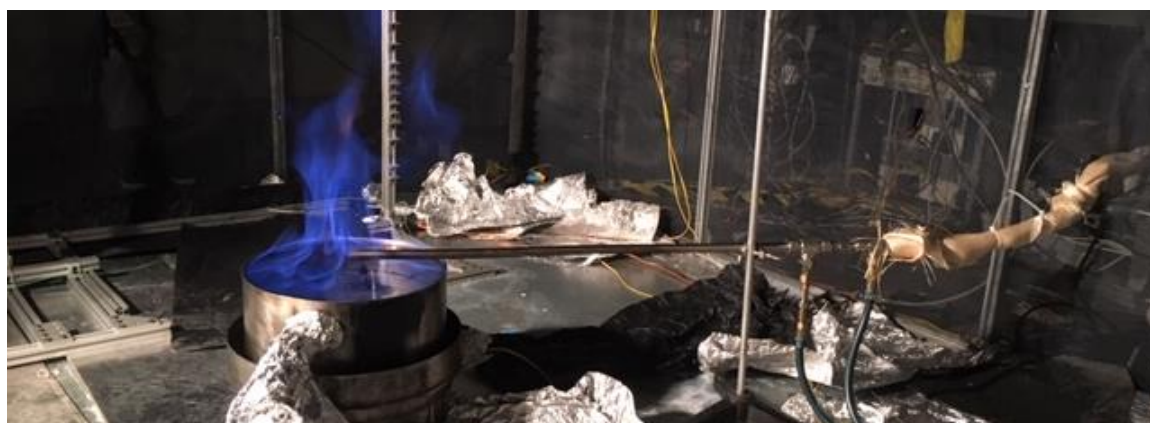


**Figure 2.** Photo of the experiment with the sampling probe in the fire (top) and schematic drawing of the flow diagram (bottom) for extractive sampling and transport of gas samples from the pool fire to the GC/MS

The sample line consisted of a 150 ml mixing chamber positioned upstream from the GC/MS. To reduce the time required to fill the mixing chamber, the sample line was split downstream into a 6.40 mm diameter “bypass” and 1.7 mm diameter “sample loop” line. For the first four minutes of sampling, gas was collected through the “bypass” line at a rate of 3.0 L/min. After the sampling path was switched to the “sample loop” line, the flow was reduced to 0.75 L/min for six minutes leading up to injection. When the sampling period was completed, the two-way valve located downstream of the sample loop line was closed. The gas sample was held within the sample loop line for one minute before injection to allow the pressure to equilibrate. Pressure was monitored using a digital pressure gauge located downstream of the GC/MS.

TCD and MS gas calibrations were conducted using commercial gas phase calibration standards. Water and Methanol calibrations were conducted using the bubbler setup shown in Fig. 3. Nitrogen, acting as a carrier gas, flowed into a liquid bath and then into the sample loop of the GC/MS. The nitrogen carrier gas flow for all calibrations was estimated to be 30 ml/min  $\pm$  3.0 ml/min. A thermocouple was placed

at the liquid surface to capture the bath temperatures needed to determine vapor pressure. Liquid bath temperatures were controlled using a heating plate positioned underneath the insulated bubbler. Liquid calibrations were conducted once the bath temperature achieved steady state (approximately 1 hour).

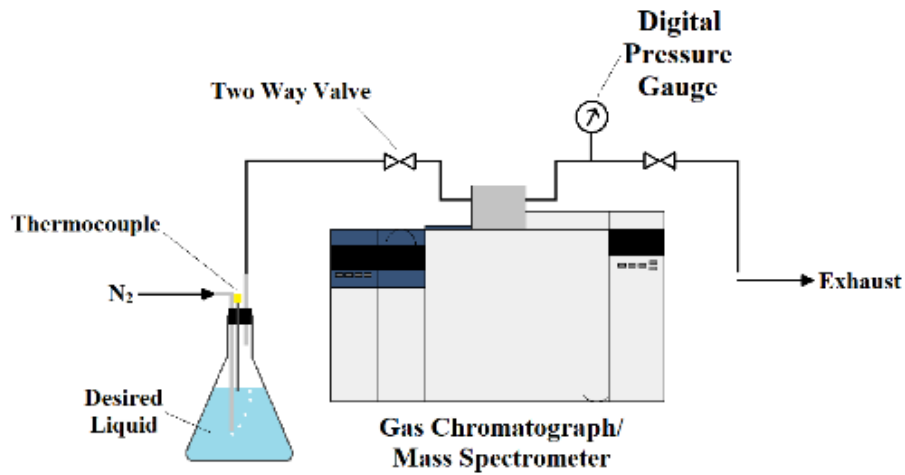


**Figure 3.** Flow diagram for bubble calibration system used for water and methanol

All measurements were repeated at least twice at each location along the centerline of the pool fire. Gas species concentration measurements made at the same location were averaged. The variance in the gas species volume fraction varied between location and species. The combined uncertainty was calculated from the standard deviation of the repeated measurements multiplied by a coverage factor of two, representing a 95 % confidence interval. A detailed description of the uncertainty analysis for the gas species measurement is described in detail elsewhere<sup>7</sup>.

### 3. Results and Discussion

Figure 4 shows two photos of the pulsing methanol pool fire. The fire shape fluctuated during its pulsing cycle with uniformly curved flame sheets present at the burner rim that rolled towards the fire centerline to form a long and narrow plume. The observed dynamic fire shape is consistent with previous descriptions<sup>3,8-9</sup>.



**Figure 4.** Images of pulsing methanol pool fire (30 cm diameter)

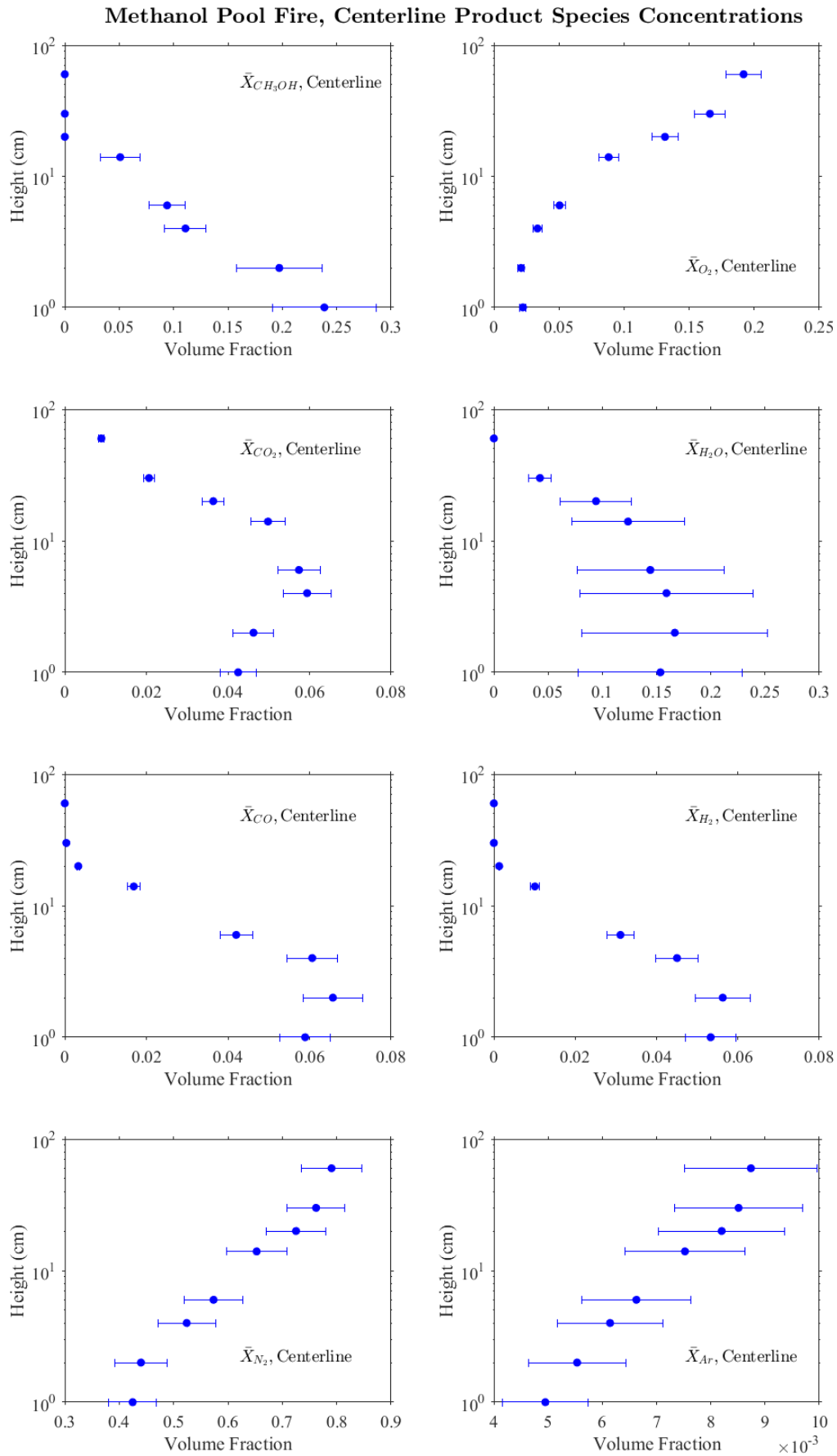
### 3.1 Gas Species Concentrations

Table 1 and Figure 5 display the averaged volume fraction,  $\bar{X}_i$ , of the significant species concentrations made at various heights along the fire's centerline and relative to the fuel surface. The species measured included the reactants, Methanol ( $\text{CH}_3\text{OH}$ ) and oxygen ( $\text{O}_2$ ), combustion products such as water ( $\text{H}_2\text{O}$ ) and carbon dioxide ( $\text{CO}_2$ ), combustion intermediates such as carbon monoxide ( $\text{CO}$ ), hydrogen ( $\text{H}_2$ ), methane ( $\text{CH}_4$ ), and inert gases such as Nitrogen ( $\text{N}_2$ ) and Argon ( $\text{Ar}$ ). As expected, the fuel volume fractions were highest, and the oxygen volume fraction was the lowest close to the fuel surface. The product species were found to have a maximum volume fraction at approximately 4 cm above the fuel surface. The intermediate gas species were found to have peaked at approximately 2 cm above the fuel surface. Inert gases were shown to increase with the distance from the fuel surface. It was also found that the gas sampled from the centerline nearly mimicked the composition of air at approximately 60 cm above the fuel surface.

**Table 1.** Concentrations of major species as a function of height relative to the pool surface

Position	$\bar{X}_{\text{CH}_3\text{OH}}$	$\bar{X}_{\text{O}_2}$	$\bar{X}_{\text{CO}_2}$	$\bar{X}_{\text{H}_2\text{O}}$	$\bar{X}_{\text{CO}}$	$\bar{X}_{\text{H}_2}$	$\bar{X}_{\text{N}_2}$	$\bar{X}_{\text{Ar}}$
1.0 cm	$24 \pm 4.8$	$2.2 \pm 0.2$	$4.3 \pm 0.4$	$15 \pm 7.6$	$5.9 \pm 0.6$	$5.3 \pm 0.6$	$42 \pm 4.4$	$0.4 \pm 0.1$
2.0 cm	$20 \pm 3.9$	$2.1 \pm 0.2$	$4.6 \pm 0.5$	$17 \pm 8.5$	$6.6 \pm 0.7$	$5.6 \pm 0.7$	$44 \pm 4.8$	$0.6 \pm 0.1$
4.0 cm	$11 \pm 1.9$	$3.4 \pm 0.3$	$5.9 \pm 0.6$	$16 \pm 8.0$	$6.1 \pm 0.6$	$4.5 \pm 0.5$	$52 \pm 5.3$	$0.6 \pm 0.1$
6.0 cm	$9.4 \pm 1.7$	$5.1 \pm 0.5$	$5.7 \pm 0.5$	$14 \pm 6.8$	$4.2 \pm 0.4$	$3.1 \pm 0.3$	$57 \pm 5.3$	$0.7 \pm 0.1$
14 cm	$5.1 \pm 1.9$	$8.8 \pm 0.8$	$5.0 \pm 0.4$	$12 \pm 5.2$	$1.7 \pm 0.2$	$1.0 \pm 0.1$	$65 \pm 5.5$	$0.8 \pm 0.1$
20 cm	*	$13 \pm 1.0$	$3.6 \pm 0.3$	$9.4 \pm 3.3$	$0.3 \pm 0.0$	$0.1 \pm 0.0$	$72 \pm 5.4$	$0.8 \pm 0.1$
30 cm	*	$17 \pm 1.2$	$2.1 \pm 0.1$	$4.3 \pm 1.1$	Trace	*	$76 \pm 5.3$	$0.9 \pm 0.1$
60 cm	*	$19 \pm 1.4$	$0.9 \pm 0.1$	*	Trace	*	$79 \pm 5.5$	$0.9 \pm 0.1$

\* Species not detected; Trace indicates concentrations less than 1000 ppm



**Figure 5.** Volume fraction of major gas species as a function of height relative to the pool surface with uncertainty defined as the standard deviation of the repeated measurements with a coverage factor of 2

#### 4. Conclusion

In summary, time-averaged local measurements of gas species concentrations were made to characterize the structure of a 30 cm diameter, methanol, pool fire steadily burning in a quiescent environment. These local measurements are essential to providing insight into the complex dynamics and chemical structure of medium-scale pool fires. It is anticipated that the data will be useful for model validation.

#### 5. Acknowledgments

The authors would like to acknowledge Kimberly Harris of the Gas Sensing Metrology Group at NIST, who assisted in the developing the species calibration method used in the study.

#### References

- <sup>1</sup> K. McGrattan, S. Hostikka, R. McDermott, J. Floyd, C. Weinschenk, and K. Overholt. *Fire Dynamics Simulator, Technical Reference Guide*. National Institute of Standards and Technology, Gaithersburg, Maryland, USA, and VTT Technical Research Centre of Finland, Espoo, Finland, sixth edition, September 2013. Vol. 1: Mathematical Model; Vol. 2: Verification Guide; Vol. 3: Validation Guide; Vol. 4: Software Quality Assurance.
- <sup>2</sup> S.J. Fischer, B. Hardouin-Duparc, and W.L. Grosshandler. The structure and radiation of an ethanol pool fire. *Combustion and flame*, 70(3): 291–306, 1987.
- <sup>3</sup> A. Hamins and A. Lock. *The Structure of a Moderate-Scale Methanol Pool Fire*. US Department of Commerce, National Institute of Standards and Technology, 2016.
- <sup>4</sup> A. Hamins, M. Klassen, J. Gore, S. Fischer, and T. Kashiwagi. Heat Feedback to the Fuel Surface in Pool Fires, *Combust. Sci. Tech.*, 97, 37-62 (1993).
- <sup>5</sup> A. Hamins, M. Klassen, J. Gore, T. and Kashiwagi, *Estimate of Flame Radiance via a Single Location Measurement in Liquid Pool Fires*, *Combustion and Flame*, 86:223-228 (1991).
- <sup>6</sup> A. Hamins, T. Kashiwagi, and R. Buch, *Characteristics of Pool Fire Burning, in Fire Resistance of Industrial Fluids*, ASTM STP 1284 (Eds: G. Totten and J. Reichel), American Society for Testing and Materials (ASTM) Publication Number 04-012840-12, W. Conshocken, PA, pp. 15-41 (1995).
- <sup>7</sup> A.Lock, M. Bundy, E.L. Johnsson, A. Hamins, G.K. Ko, C. Hwang, P. Fuss, and R. Harris, *Experimental Study of the Effects of Fuel Type, Fuel Distribution, and Vent Size on Full-Scale Underventilated Compartment Fires in an ISO 9705 Room*, NIST Technical Note 1603, National Institute of Standards and Technology, Gaithersburg, MD, October 2008.
- <sup>8</sup> E.J. Weckman and A. Sobiesiak, *The Oscillatory Behavior of Medium-Scale Pool Fires, Proceedings of the Twenty-Second Sym. (Int.) on Combustion*, The Combustion Institute, 1299-1310 (1988).
- <sup>9</sup> H. R. Baum, and B. J. McCaffrey, *Fire Induced Flow Field - Theory and Experiment, Proceedings of the Second International Symposium on Fire Safety Science*, Hemisphere, New York, 129-148 (1989).